Catalysis Today 175 (2011) 238–244

Contents lists available at ScienceDirect

Catalysis Today

journal homepage: www.elsevier.com/locate/cattod

N_2O decomposition over Fe-FER: A Mössbauer study of the active sites

E. Tabor [a], K. Závěta [b], N.K. Sathu [a], A. Vondrová [a], P. Sazama [a], Z. Sobalík [a,*]

[a] J. Heyrovský Institute of Physical Chemistry of the ASCR, v. v. i., Dolejškova 3, CZ-182 23 Prague 8, Czech Republic
[b] Joint Laboratory for Mössbauer Spectroscopy, Faculty of Mathematics and Physics, Charles University in Prague, V Holešovičkách 2, CZ-180 00 Prague 8, Czech Republic

ARTICLE INFO

Article history:
Received 31 October 2010
Received in revised form 24 February 2011
Accepted 12 April 2011
Available online 13 May 2011

Keywords:
Iron ferrierites
N_2O decomposition
Cationic sites
Mössbauer spectroscopy

ABSTRACT

Iron ferrierites with low iron content (Fe/Al between 0.018 and 0.072) were used as model catalysts to evaluate the participation of individual iron species, with special interest in the role of iron in β cationic sites, for formation of active sites for N_2O decomposition. Despite low iron content, the catalysts with prevailing iron located in β sites of two types exhibited high conversions of N_2O and activity increase with increase of iron loading. These results indicate formation of the active iron species already at very low concentrations, while at higher concentration level would part of the iron enter also into less active positions. Semi-quantitative analysis of the TOF values of individual iron centers was done using the recently established Mössbauer parameters of the Fe(II) parameters for individual iron cationic species, i.e. β (β-1 and β-2) and α sites [1]. The evaluation of the TOF presents a new support for the role of iron in β sites in N_2O decomposition and further indicates similar role of both β-1 and β-2 sites in formation of the Fe···Fe active site.

1. Introduction

Due to their unique redox properties, iron zeolites exhibit high catalytic activity in several reactions such as selective catalytic reduction of nitrogen oxide by hydrocarbons [2–4], hydroxylation of benzene by N_2O [5,6], simultaneous reduction of NO and N_2O by NH_3 [7], and direct N_2O decomposition [8,9]. Recently, it was shown that iron ferrierites (Fe-FER) with low iron loading ($Fe/Al < 0.1$) exhibited high catalytic activity in direct N_2O decomposition without the addition of NO [10]. Many studies have been devoted to the determination of the nature of iron active sites in iron zeolites [10–14]. It was suggested that divalent iron plays an important role in N_2O decomposition [10,13–15]. Nevertheless, the detailed structure of iron active sites is still a matter of discussion. DFT calculations have indicated that the active sites, responsible for superior activity of ferrierite among the series of high silica pentasil zeolites in N_2O decomposition at the lower temperature region, contain two adjacent β sites facing each other across the channel [10]. These also identified the reason for the formation of such unique arrangement in iron ferrierites, i.e. optimal structural topology of the ferrierite and Al distribution providing for stabilization of iron in β sites with optimal Fe–Fe distance of 7.4 Å [13]; further in the text referred to as the Fe···Fe site. It was shown that when two Fe(II) cations accommodated in two adjacent β sites can collaborate then the N–O cleavage is facile (barriers are only 9.4 and 12.3 kcal/mol for the β-1 and β-2 sites, respectively) [13]. The structures of particular cationic positions were described in details elsewhere [1,12,13].

Mössbauer spectroscopy, due to its unique possibility to recognize all iron forms present in the investigated sample, is an excellent tool for studying oxidation state and coordination of iron species [1,14–18]. The principal advantage of this method is the possibility to recognize all iron forms present in the investigated sample, while other method (UV–Vis, EPR, FTIR, etc.) are restricted only to some of the iron forms and oxidation states (e.g. EPR), or are lacking in the sensitivity down to such low concentration region (e.g. EXAFS). Nevertheless, the majority of Mössbauer studies characterizing iron zeolites was focused on MFI structure and mostly investigated catalysts with relatively high iron loading [15,16]. Only several papers were devoted to iron ferrierites [18–20]. In addition, the authors investigated catalysts with relatively high iron loading ($Fe/Al > 0.1$). As a result, various types of iron species in oversaturated Fe zeolite were characterized and it made Mössbauer analysis more complex.

Identification of the active species is complicated by the fact that obviously only part of iron present in zeolite structure, and formed namely at low iron concentration levels, plays a crucial role in N_2O decomposition [10,14,16].

Recently, we reported Mössbauer parameters of Fe(II) bonded in the individual cationic positions of ferrierites [1], which provided a new potential for detail characterization of iron species located in cationic positions at zeolites of low iron concentration, and thus open the possibility to analyze further the structure/catalytic performance of iron ferrierite in N_2O decomposition reaction.

---

[*] Corresponding author. Tel.: +420 266 053 646; fax: +420 286 582 307.
E-mail address: zdenek.sobalik@jh-inst.cas.cz (Z. Sobalík).

0920-5861/$ – see front matter © 2011 Elsevier B.V. All rights reserved.
doi:10.1016/j.cattod.2011.04.024

In this contribution, we report on such attempt for elucidation of the structure/catalytic performance relationship using iron ferrierites with very low iron content and Mössbauer spectroscopy as the principal method for monitoring of the structure of iron species.

2. Experimental

2.1. Catalyst preparation

Iron ferrierite catalysts were prepared by synthesis method based on impregnation of ammonium form of ferrierite (NH_4-FER, Tosoh, Si/Al = 8.6) by acetylacetone solution of $FeCl_3$. Then, the sample was evacuated for four hours at 100 °C and at 350 °C. After cooling to room temperature, the sample was washed with distilled water and calcined overnight under air flow at 420 °C. The preparation procedure is described in details elsewhere [18]. For all three synthesized iron ferrierite catalysts the isotopically enriched $^{57}FeCl_3$ (prepared from iron oxide with ^{57}Fe enrichment over 98% delivered by Isoflex, USA) was used. The samples with Fe/Al molar ratio 0.018, 0.036, and 0.072 were denoted as Fe-FER18, Fe-FER36, and Fe-FER72, respectively.

2.2. Catalytic activity

A fixed-bed plug flow-through micro-reactor was used for measurement of catalytic activity for N_2O decomposition. 50 mg of catalyst (0.3–0.6 mm) was placed in a U-shaped glass tube reactor (I.D. = 4 mm) between two quartz wool plugs. Before the reaction, catalysts were pre-treated at 450 °C in a flow of He for 2 h and in pure He for 1 h at 450 °C, then temperature decreased to respective N_2O decomposition test (300–450 °C). The reaction stream contains 1000 ppm of N_2O in He, with total flow rate 300 ml/min, corresponding to gas hour space velocity (GHSV) 180 000 h^{-1}. Catalytic tests were performed at atmospheric pressure and reactant flow rates were controlled by Aalborg digital mass flow controllers. A Eurotherm 3508 temperature-controller was used to control the reaction temperature. The reaction temperature was measured by a thermocouple located in the middle of the catalyst bed. The kinetic setup was constructed by using Swagelok stainless steel material; the 1/8 stainless tubing of the system was heated with thermo coils. Analysis of the gas composition at the reactor outlet was performed using an Advance Optima IR analyzer (ABB Co., Germany) for N_2O, and chemiluminescence analyzer (MLU AM) for NO and NO_2. The steady state conversion data for a catalyst has been taken as a measure of a catalyst performance.

N_2O conversions were evaluated by analyzing N_2O feed concentrations before (bypass) and after passing through the catalyst bed. The conversion was calculated using the following equation:

$$\text{Conversion}\quad(\%) = \frac{[N_2O_{\text{bypass}}]_{\text{ppm}} - [N_2O_{\text{reaction}}]_{\text{ppm}}}{[N_2O_{\text{bypass}}]_{\text{ppm}}} \times 100\%$$

Turnover frequency values (TOF, h^{-1}) were based on conversion data at temperatures between 375 and 425 °C and were defined as number of N_2O molecules decomposed per hour per one Fe ion in the individual type of cationic site. The data for concentrations of individual ion types were based on Mössbauer data and further supported by FTIR results.

2.3. Catalyst characterization

Mössbauer spectroscopy was used as the principal method of quantitative analysis of the individual iron species and for analyses of the behavior of iron species under redox conditions. Self-supporting pressed pellets of iron ferrierites having a weight of about 100 mg were used for Mössbauer measurements. The pellet was placed into a laboratory-made chamber that enabled the transport of the sample between heating region and measurement position. The transmission ^{57}Fe Mössbauer spectra were collected in vacuum at room temperature after following alternative treatments: (i) evacuation at 450 °C for 3 h (*evacuated sample*); (ii) evacuation at 450 °C for 3 h followed by oxidation with dioxygen (13 kPa) at 450 °C for 30 min and evacuation (*O_2-oxidized sample*); (iii) evacuation at 450 °C for 3 h followed by oxidation with N_2O (13 kPa) at 250 °C for 30 min and evacuation (*N_2O-oxidized sample*). The maximum velocity of the source was 12 mm/s and the velocity scale was calibrated using α-Fe. The spectra were fitted into Lorentzian-shaped components using MossWinn software. The corresponding Mössbauer parameters, i.e. isomer shift (IS), quadrupole splitting (QS), and magnetic hyperfine field (B_{hf}) were then ascribed to individual iron species in iron ferrierites. The identification and semi-quantitative evaluation of the Fe(II) in α, β-1 and β-2 cationic sites was done using parameters of IS and QS as established previously [1].

In order to support the results obtained from Mössbauer spectroscopy, FTIR and UV–Vis spectroscopies were employed. FTIR spectra of iron ferrierite catalysts dehydrated at 450 °C for 3 h were collected with the resolution of 2 cm^{-1} at room temperature in a glass vacuum cell equipped with six position carousel holder and NaCl windows using a Nexus 670 FTIR (Thermo Nicolet) spectrometer. The samples for FTIR measurements were prepared as self-supporting wafers with thickness between 5 and 10 mg/cm^2. The presence of iron in cationic positions of ferrierite structure was determined in the "skeletal transmission window" of FTIR spectrum (a region between 940 and 860 cm^{-1}), where the antisymmetric T–O–T stretching lattice vibrations perturbed by the divalent ion were observed. The band position in the transmission window was identified by a Fourier self-deconvolution procedure (OMNIC 4.1 software). Final data processing was carried out using the OriginPro 7.5 software (MicroLab Corporation, USA) analyzing the spectra in the region from 980 to 820 cm^{-1}. UV–Vis spectra of the catalysts dehydrated under vacuum (450 °C for 3 h) were collected in the range between 10 000 and 50 000 cm^{-1} using a Perkin-Elmer Lambda 950 spectrometer equipped with Spectralon^{TM} integration sphere. WinLab software was applied to recalculate the spectra using the Schuster–Kubelka–Munk equation [21].

3. Results and discussion

3.1. Catalytic results

The results of N_2O decomposition over FeFER18, FeFER36, and FeFER72 as a function of the reaction temperature are presented in Fig. 1. All investigated catalysts operate at temperatures above 350 °C, the FeFER36 and FeFER72 samples have a noticeable activity at even lower temperatures. The conversion of N_2O was increasing with iron content in the whole temperature region (Fig. 1).

Data for activity increase in the all three samples were obtained in the temperature window between 325 and 450 °C, while at temperatures below and above this temperature window would be influenced by either two low conversion data for the FeFER18, or would be deformed by activity over 50% of the FeFER72 sample. Thus the N_2O conversion at the used temperature window was between 4 and 40% for all the Fe-FER catalysts studied. The activity in this region increases and this increase is roughly proportional to the increasing concentration of the iron in the FeFER18 and FeFER36 samples. Further increase in the concentration of iron from 62 to 123 μmol/g for the FeFER36 and FeFER76 samples, respectively, resulted in an increase in N_2O conversion, which does not correlate with two times higher iron loading in the sample FeFER72. Using these conversion data the formal TOF values were calculated for

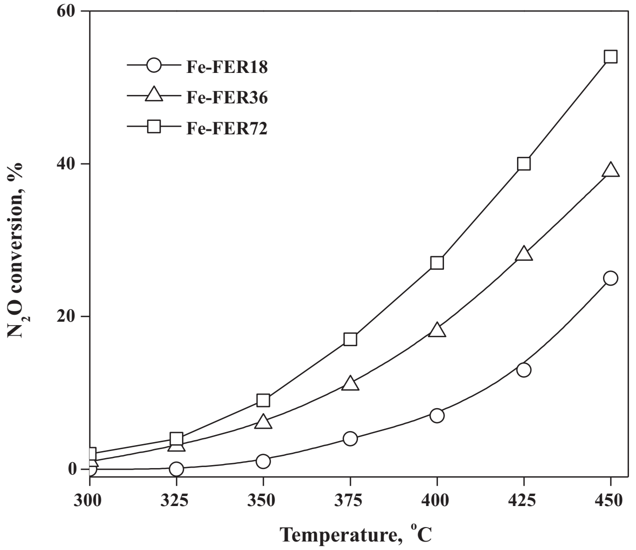

Fig. 1. Temperature dependence of N_2O decomposition on Fe-FER18, Fe-FER36, and Fe-FER72.

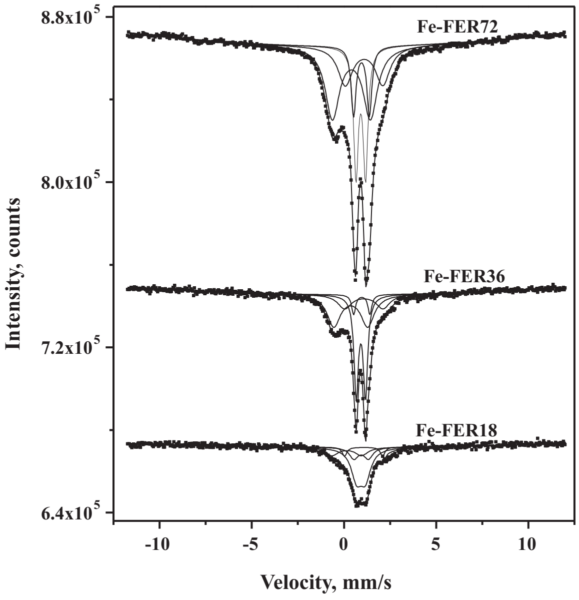

Fig. 2. Mössbauer spectra of Fe-FER18, Fe-FER36, and Fe-FER72 after oxidation by O_2 together with their fits.

the individual iron cation concentration as analyzed by Mössbauer spectroscopy analysis, see further.

3.2. Mössbauer spectroscopy

In accordance with our recent results [1], the concentration of individual iron species were analyzed based on the determined Mössbauer parameters, i.e. divalent iron in α cationic position was characterized by following parameters: IS = 1.02 mm/s; QS = 2.02 mm/s; the two components described by IS = 0.92 mm/s; QS = 0.44 mm/s and IS = 0.94 mm/s; QS = 0.70 mm/s were assigned to iron in β-1 and β-2 sites in Fe-FER, respectively.By such analysis the changes in the occupation of individual cationic positions by iron ions with the increasing of iron loading could be semi-quantitatively determined and follows the usual pattern showing preference for β sites occupation at low cation concentration. Accordingly, in the sample with the lowest iron loading (Fe-FER18) the iron in α site presents only a minority species, and thus the relative contribution of the prevailing iron in β sites is well above to 80%. Preference for occupation of the β sites at samples of lower content of divalent cations is generally supported by literature data, showing the general trend of increase of the occupation of the α position with increasing iron content [11]. On the other hand, the ratio between occupations of the two alternative β sites is strongly changing. In the case of the sample with the lowest iron loading Fe-FER18 the population of the individual β sites is nearly equal (41% of iron present is occupying β-1, and roughly 42% the position β-2). A similar trend was also observed in the case of Fe-FER36, containing 75% of Fe(II) located in β sites, and 25% of iron in α sites. Nevertheless, it was accompanied namely by relative increase of the β-2 position and less by β-1 (31% of β-1 and 44% of β-2). With increasing the iron content the occupation of the α site further increases and in the catalyst with the highest iron loading (Fe-FER72) and reached nearly the level of the β sites and about 36% of iron present was situated in the β and 32% in α position. The rest of the iron presented a stable Fe(III) containing sites obviously detrimental for the catalytic activity in N_2O decomposition. This additional iron species were characterized by Mössbauer parameters of IS = 0.30 mm/s; QS = 1.87 mm/s. This spectral component appeared only in the samplewith the highest iron content, i.e. in Fe-FER72, and was assigned to dinuclear iron complex,which is not decomposed during evacuation at 450 °C or to isolated extra-framework Fe(III) ions [1,18]. The rough estimation of the amount of iron located in β-1, β-2, and α in these samples, based on quantifying of the Mössbauer data, is included in Table 1. Without doubts, the obtained data are only semi-quantitative, as done by the limited potential of the Mössbauer fitting approaches for exact quantitative data. Nevertheless, it would provide a background for the relative evaluation of the tendencies in the change of the activity with iron content. It also positively showed the basic difference in the occupation of the β-1 and β-2 sites. Namely, while the amount of β-1 is nearly stable with increasing iron concentration, the increasing amount of iron is accommodated mostly in the β-2, and later in the α cationic positions. Nevertheless, the Mössbauer spectroscopy could not indicate either the proportion of β sites situated in the double β site or isolated β sites or the participation of the β-1 and the β-2 sites in the formation of the catalytically active double β site.

Mössbauer spectra of Fe-FER18, Fe-FER36, and Fe-FER72 after treatment with O_2 are presented in Fig. 2 and the corresponding Mössbauer parameters are collected in Table 2.

The Mössbauer spectrum of Fe-FER18 after oxidation by O_2 was deconvoluted into four components. Three of them are characteristic for iron unperturbed by the treatment in oxygen and located in cationic positions α, β-1, and β-2 [1], and thus presents a part of these sites which resist oxidation under used conditions. At present, there is no interpretation for the structural features controlling the response of the individual β sites to oxidation by molecular oxygen. The third component, exhibiting the IS value lower than 0.7 mm/s and indicating the presence of Fe(III) [10,14,17], was produced by oxidative treatment, and is characterized by Mössbauer parameters IS = 0.12 mm/s; QS = 1.19 mm/s. The high value of QS points to lower symmetry around iron Fe(III) center. The analysis of the Mössbauer spectrum of Fe-FER18 after treatment with O_2 showed that only part of Fe(II) in cationic position was oxidized by O_2. Approximately 80% of Fe(II) of Fe-FER18 in cationic positions remained resistant to oxidation by O_2. The comparison of the fitting results for dehydrated Fe-FER18 with that after O_2 treatment (see Table 1) indicates that iron located in β sites are more resistant against transformation by O_2 than iron located in α sites.

Fe-FER36 after oxidation by O_2 was deconvoluted into four components showing that again the prevailing part of iron (∼80%) was not oxidized by O_2 and were under such conditions stable as Fe(II)

Table 1
Concentration in μmol of Fe/g of sample, of iron species as analyzed by Mössbauer; FTIR results in brackets.

	Fe-FER18 [μmol/g]			Fe-FER36 [μmol/g]			Fe-FER72 [μmol/g]		
	Evacu.[a]	O_2[b]	N_2O[c]	Evacu.[a]	O_2[b]	N_2O[c]	Evacu.[a]	O_2[b]	N_2O[c]
β-1	12	12	–	17	17	–	14	13	–
β-2	14	12	–	29	23	–	31	27	–
β-1 + β-2	26 (25)	24	–	46 (42)	40	–	45 (42)	40	–
α	6 (7)	2	–	16 (20)	8	–	40 (42)	25	–
Fe(III) species	–	6	32	–	14	62	38	58	123

[a] Evacuated sample.
[b] O_2-oxidized sample.
[c] N_2O-oxidized sample.

Table 2
Mössbauer parameters Fe-FER samples oxidized by oxygen.

Catalyst	Isomer shift (mm/s)	Quadrupole splitting (mm/s)	Spectral contribution (%)	Iron species	Oxidation state of Fe ions
Fe-FER18	0.95	0.49		β-1	Fe(II)
	0.94	0.71	33	β-2	Fe(II)
	1.01	2.01	6	α	Fe(II)
	0.12	1.19	20	FeO_x	Fe(III)
Fe-FER36	0.92	0.49	28	β-1	Fe(II)
	0.96	0.78	37	β-2	Fe(II)
	1.07	2.08	13	α	Fe(II)
	0.28	1.69	22	FeO_x	Fe(III)
Fe-FER72	0.92	0.46	10	β-1	Fe(II)
	0.90	0.70	22	β-2	Fe(II)
	1.10	2.04	19	α	Fe(II)
	0.36	2.03	49	FeO_x	Fe(III)

in β cationic sites and to lower extend in α sites. The produced oxidized iron species have Mössbauer parameters IS = 0.30 mm/s; QS = 1.69 mm/s, i.e. typical for Fe(III), nevertheless different from the species produced in sample at lower concentration level (for Fe-FER18; IS = 0.12 mm/s; QS = 1.19 mm/s).

The sample with the highest iron concentration used (Fe-FER72) displayed similar behavior. However, in this sample some amount of Fe(III) was present already before O_2 treatment. The analysis of the Mössbauer spectrum of the sample after treatment with O_2 showed that the components characteristic for Fe(II) in α and β cationic positions did not disappear. In Fe-FER72 the amount of Fe(II) located in cationic sites after O_2 treatment decreased from 67% to 54%. The remaining part of iron (spectral contribution of Mössbauer spectrum 46%) present in Fe-FER72 characterized by a doublet with IS = 0.36 mm/s; QS = 2.06 mm/s was assigned to Fe(III).

In all investigated samples O_2 treatment led to the oxidation of nearly the same proportion of the iron cations, i.e. presenting about 20% of the Fe(II) in the samples. These results clearly suggest that only part of the iron located in cationic positions could be transformed into oxidized form by molecular oxygen. It further indicates lower resistance of α sites to O_2 oxidation in comparison with iron located in β sites (β-1 + β-2) (see Table 1).

The Fe(III) species formed after O_2 treatment in the investigated samples exhibited a slightly different value of QS. The QS value determines the symmetry around the iron ions, and as a rule, the higher value of QS the lower symmetry around Fe ion observed. Based on this correlation, the decreasing of the symmetry of Fe(III) species after oxidation by molecular oxygen could be tentatively suggested with increasing of Fe loading in the studied iron ferrierites. The nature of the oxidized products has been already tentatively assigned others to Fe(III) mono or dinuclear oxo-complexes [14,17], nevertheless more analysis would be necessary for convincing structural characterization of these Fe(III) oxo-species.

N_2O proved to be a more potent oxidation agent for Fe(II)-FER at the low concentration levels studied, and accordingly most of the present Fe(II) in cationic positions was oxidized by N_2O under mild conditions. Consequently, oxidation by N_2O dramatically changed the Mössbauer spectra of the investigated samples. The Mössbauer spectra of Fe-FER18, Fe-FER36, and Fe-FER72 after treatment with N_2O are presented in Fig. 3 together with their fits. The corresponding Mössbauer parameters are collected in Table 3.

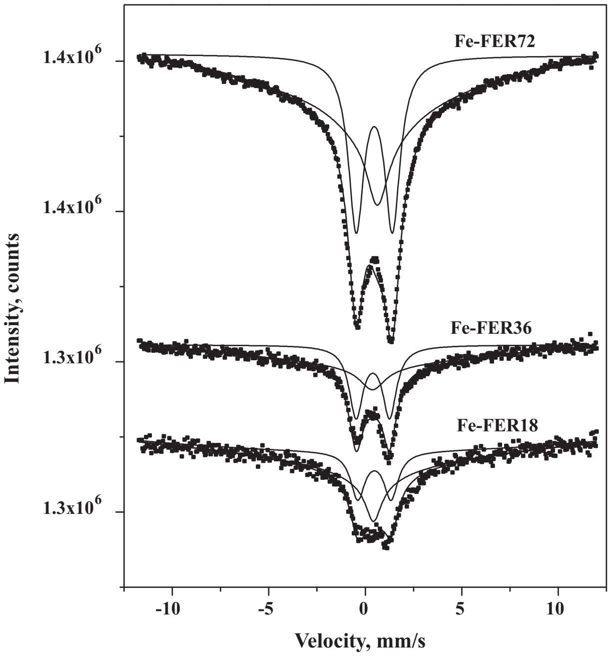

Fig. 3. Mössbauer spectra of Fe-FER18, Fe-FER36, and Fe-FER72 after oxidation in N_2O together with their fits.

Iron present in the dehydrated Fe-FER18 was fully oxidized from Fe(II) to Fe(III). Two species containing Fe(III) were identified with different Mössbauer parameters. The component with IS = 0.43 mm/s; QS = 1.87 mm/s has relatively high value of QS that indicates higher symmetry around iron centers [14]. A dominant

Table 3
Mössbauer parameters of Fe-FER18, Fe-FER36, and Fe-FER72 N_2O-oxidized.

Catalyst	Isomer shift (mm/s)	Quadrupole splitting (mm/s)	B_{hf} (T)	Spectral contribution (%)	Oxidation state of Fe ions
Fe-FER18	0.47	1.70		28	Fe(III)
	0.43		42.00	72	Fe(III)
Fe-FER32	0.39	1.73		35	Fe(III)
	0.45		42.00	65	Fe(III)
Fe-FER72	0.43	1.86		34	Fe(III)
	0.36		42.00	66	Fe(III)

(∼64%) broad signal present in Mössbauer spectrum of Fe-FER18 characterized by IS = 0.21 mm/s and B_{hf} = 51 T can be described as a relaxation component and ascribed to various magnetically ordered type of iron oxygen complexes formed after interaction with N_2O. The presence of this component in Mössbauer spectrum indicates the paramagnetic hyperfine interactions in iron zeolites, already reported in several papers [15,17,22]. These studies showed that treatment of iron zeolites with N_2O leads to the formation and stabilization of the active form of oxygen on iron centers. The matter of discussion is the location of active form of oxygen. As stressed already, results from DFT calculation presented by Sklenák et al. suggested that the cooperation of two Fe(II) located in β cationic position in the opposite site of eight-membered ring channel can play essential role in N_2O activation [13]. Using Mössbauer spectroscopy it was shown that Fe(II) plays the essential role in the formation of active oxygen [14,15]. Nevertheless, after absorption of N_2O on Fe-FER under atmosphere pressure is not possible to distinguish in Mössbauer spectrum the affinity of particular Fe cationic positions to N_2O oxidation.

In the case of the samples with higher iron loading, i.e. Fe-FER36 and Fe-FER72, the treatment with N_2O led to nearly complete oxidation of Fe(II) to Fe(III). In both cases the component characteristic for paramagnetic hyperfine interaction was observed. Prevailing part of Fe(III) was present as magnetically ordered iron (the parameters see Table 3). The IS and QS values are characteristic for Fe(III) and the quite high value of QS points to the low symmetry of the oxidized iron species [14,22].

3.3. FTIR and UV–Vis spectroscopy

FTIR and UV–Vis spectroscopy were used to support the analysis by Mössbauer spectroscopy by confirming the presence of iron located in cationic positions and semi-quantitative evaluation of Fe(II) in β and α positions (FTIR) as well as the presence of iron oxides in samples with higher iron content (UV–Vis).

FTIR spectra of investigated samples are collected in Fig. 4. The evaluation of the distribution of iron at particular cationic position in Fe-FER18, Fe-FER36, and Fe-FER72 analyzed by Mössbauer and IR spectroscopy is shown in Table 1.

The analysis of FTIR spectra at the region of T–O–T perturbed skeletal vibrations of Fe-FER18, Fe-FER36, and Fe-FER72 have shown the bands at 913–910 cm^{-1} and 936 cm^{-1} assigned to Fe(II) in β and α sites, respectively [11]. In the whole concentration range the occupation of β sites prevails but the relative occupation of iron in α sites is steadily increasing.

UV–Vis spectra of dehydrated Fe-FER18, Fe-FER32, and Fe-FER72 samples confirmed the absence of oxidic forms of iron in all investigated samples. In the case of the sample Fe-FER72 only negligible amount of Fe(III) is present, which could be assigned to FeO_x species.

3.4. Structure/catalytic activity relationship

The catalytic results have shown that the iron ferrierites with low iron loading exhibited appreciable activity for N_2O conversion already at temperatures above 350 °C. It was found that iron in cationic positions namely in Fe···Fe pairs, should be expected to play a crucial role in N_2O decomposition over Fe-FER at lower temperature region and without the accelerating NO in the feed [10,11,13]. As convincingly presented by this DFT analysis such optimal arrangement of the iron species could be reached exclusively in the β cationic positions. On the other hand, estimation of the preference of the iron cation for occupation of such local arrangement, and not the isolated β positions, as well as the possibility of participation of both β type sites in the formation of the optimal catalytic structures, could be based only on statistical models. Such model should take into consideration Al distribution in the framework, as well as preference of the exchange of Fe pairs in the neighboring empty cationic positions of the β type. The analysis of the correlation between the occupation of individual cationic positions by iron cations and the catalysts performance with increasing iron content should provide some background for such analysis.

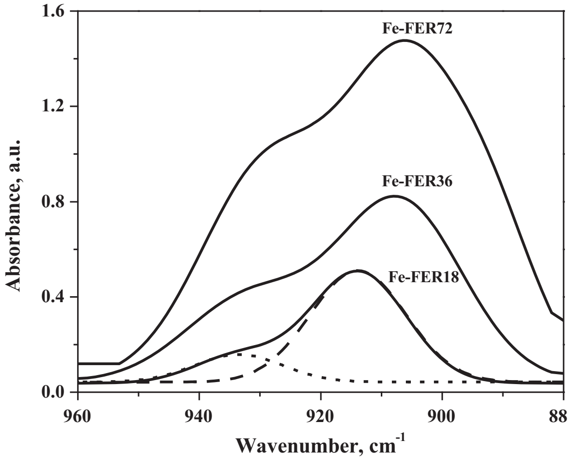

Fig. 4. FTIR spectra of dehydrated Fe-FER18, Fe-FER36, and Fe-FER72 in the transmission window region. (——) experimental, (......) α sites and (– – –) β sites.

Mössbauer spectroscopy measurements, as well as FTIR results, confirmed the prevalence of iron located in cationic β-1, β-2 and α positions in the whole concentration range of the study. Even in the sample Fe-FER72 the majority (70%) of iron is located in cationic positions. The amount of iron located in β-1 cationic position is nearly the stable for all samples, probably due to limited amount of such local Al arrangement and thus due to “saturation” of this cationic position. This is supported by the expected imbalance between content of the two β sites and very limited amount of this cationic site in the studied ferrierite [12]. With the increasing of iron content the additional iron cations are then accommodated in the empty β-2 and α sites.

The individual cationic sites exhibit different redox properties and while all Fe(II) sites are oxidized to Fe(III) after N_2O treatment, only partial oxidation of Fe(II) in the cationic positions has been found after treatment in O_2. The analysis of the relationship

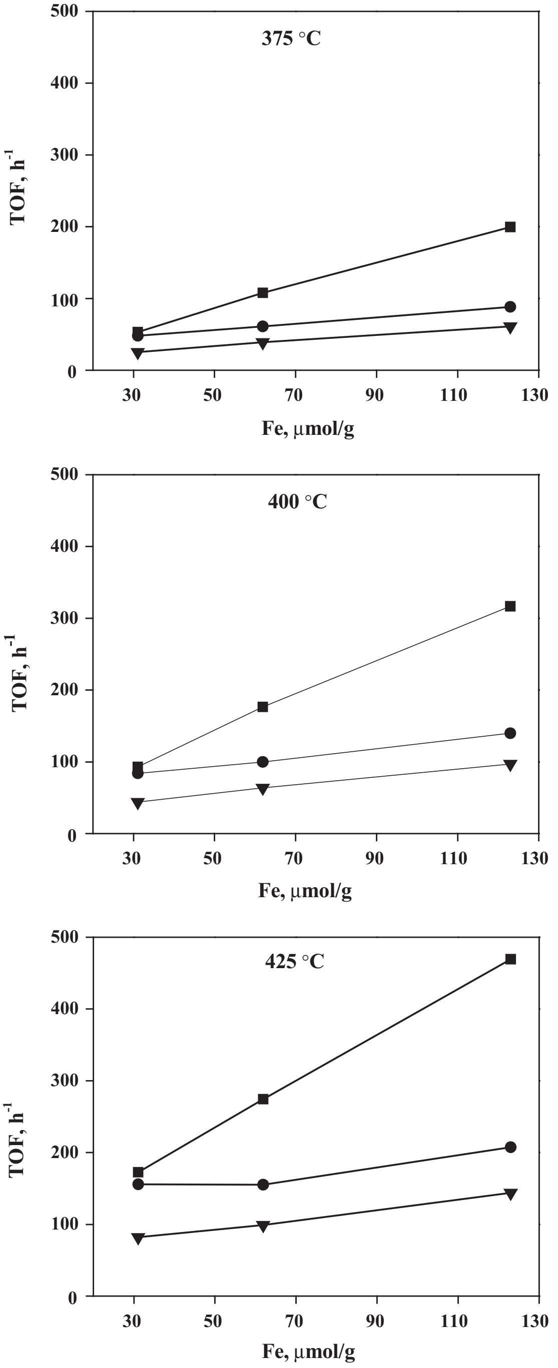

Fig. 5. Calculated TOF values for individual iron cationic sites of Fe-FER18, Fe-FER36, and Fe-FER72 at reaction temperatures between 375 and 425 °C. (■) $TOF_{\beta\text{-}1}$, (●) $TOF_{\beta\text{-}2}$, and (▼) TOF_{β}.

between the iron speciation and the catalytic performance for N_2O decomposition would evidence that the non-cationic iron sites are inferior towards the N_2O decomposition activity. The structural and catalytic results would present an additional direct experimental evidence for participation of Fe located in β positions in the formation of the active sites for N_2O decomposition.

To further analyze the structural/catalytic performance relationship the kinetic data were treated with a simplified assumption that only one type of the iron site or their combination participate on the formation of the active site, and the contribution of the other to the total conversion is negligible. Therefore, $TOF_{\beta\text{-}2}$ or $TOF_{\beta\text{-}2}$, and TOF_{β} corresponding to the individual iron sites or their combination, respectively, in dependence on the concentration of the individual iron sites were calculated using conversion data between 375 and 425 °C. The respective TOF values are summarized in Fig. 5.

The absolute values of the TOF calculated for different reaction temperatures are naturally different; nevertheless the general trends in all these temperatures are similar: neither of the TOF values obtained presents a constant value at the concentration range studied as would be symptomatic of one isolated cationic site as the sole active species in the activity for N_2O decomposition. The formal $TOF_{\beta\text{-}1}$ values exhibit unrealistic increasing trend in agreement with the limiting β-1 concentration reached already at low iron concentration. On the other hand the $TOF_{\beta\text{-}2}$ as well as the TOF_{β}, i.e. the value calculated for a sum of the iron concentration in both β sites, present slightly but systematically increasing values. Moreover, in accordance with the previous analysis [13], the occupation of α site, which is due to its position in the FER structure isolated and could not provide the double iron site with optimal orientation, is detrimental for the catalytic activity for N_2O decomposition.

Thus, while the catalytic activity is consistently connected with the presence of iron in the cationic sites of the β type, the structural arrangement for high N_2O decomposition activity would necessitate the specific Fe···Fe arrangement. Moreover, while the β-1 site is saturated at very low iron ion exchange, the β-2 is responsible for accommodation of the most of the iron cation at higher iron exchange.

On the other hand both the $TOF_{\beta\text{-}2}$ as well as the sum of TOF_{β} are consistently increasing in the whole concentration and temperature regions. That would be in agreement with equivalence of both β sites in formation of the active Fe···Fe sites, and the steadily increasing relative occupation of the Fe···Fe sites with increasing the iron content in the sample as well as the occupation of β sites.

Thus, the relative proportion of the double Fe···Fe site on the all occupied β sites would increase by a factor of two for iron concentration increase between 30 and 120 μmol Fe per g of the catalyst. In accordance with that no basic difference could be indicated between iron in β-1 and β-2 positions in formation of the active sites for N_2O decomposition over Fe-FER.

4. Conclusion

Combination of the catalytic results in N_2O decomposition with the semi-quantitative results of Mössbauer analysis of the iron speciation in the Fe-FER provided an additional experimental evidence for the decisive role of cations regularly coordinated in the cationic sites of ferrierite for N_2O decomposition over Fe-FER has been obtained.

It also provided background for discussion of the relationship between the types of iron species in Fe-FER and their catalytic activity in N_2O decomposition. It showed the increasing probability of the double iron occupation at the adjacent β cationic sites with increasing iron content without special preference for participation of iron situated in either β-1 or β-2 sites.

Acknowledgments

This work was financially supported by the Grant Agency of the Academy of Sciences of the Czech Republic (Project No. KAN100400702), the Grant Agency of the Czech Republic (Project No. 203/09/1627), the Center of Excellence IDECAT (Project No. NMP3-CT-2005-011730), and the Ministry of Education, Youth and Sports of the Czech Republic (Project No. VZ 0021620834). P.S. acknowledges support of the Czech Science Foundation, Project No. GP203/08/P593.

References

[1] E. Tabor, K. Závěta, N.K. Sathu, Z. Tvarůžková, Z. Sobalík, Catal. Today (2010), doi:10.1016/j.cattod.2010.09.017.
[2] A.L. Kustov, T.W. Hansen, M. Kustova, C.H. Christensen, Appl. Catal. B 76 (2007) 311.
[3] L. Čapek, L. Vradman, P. Sazama, M. Herskowitz, B. Wichterlová, R. Zukerman, R. Brosius, J.A. Martens, Appl. Catal. B 70 (2007) 53.
[4] A.M. Frey, S. Mert, J. Due-Hansen, R. Fehrmann, C.H. Christensen, Catal. Lett. 130 (2009) 1.
[5] L.V. Pirutko, V.S. Chernyavsky, A.K. Uriarte, G.I. Panov, Appl. Catal. A 227 (2002) 143.
[6] A. Ribera, I.W.C.E. Arends, S. de Vries, J. Pérez-Ramírez, R.A. Sheldon, J. Catal. 195 (2000) 287.
[7] B. Coq, M. Mauvezin, G. Delahay, J.B. Butet, S. Kieger, Appl. Catal. B 27 (2000) 173.
[8] I. Melian-Cabrera, C. Mentruit, J.A.Z. Pieterse, R.W. van den Brink, G. Mul, F. Kapteijn, J.A. Moulijn, Catal. Commun. 6 (2005) 301.
[9] M. Mauvezin, G. Delahay, B. Coq, S. Kieger, J.C. Jumas, J. Olivier-Fourcade, J. Phys. Chem. B 105 (2001) 928.
[10] K. Jíša, J. Nováková, M. Schwarze, A. Vondrová, S. Sklenák, Z. Sobalík, J. Catal. 262 (2009) 27.
[11] B. Wichterlová, Z. Sobalík, J. Dědeček, Appl. Catal. B 41 (2003) 97.
[12] L. Benco, T. Bucko, R. Grybos, J. Hafner, Z. Sobalík, J. Dědeček, S. Sklenák, J. Hrušák, J. Phys. Chem. C 111 (2007) 9393.
[13] S. Sklenák, P.C. Andrikopoulos, B. Boekfa, B. Jansang, L. Jana Nováková, T. Benco, J. Bucko, J. Hafner, Z. Dědeček, Sobalík, J. Catal. 272 (2010) 262.
[14] K.A. Dubkov, N.S. Ovanesyan, A.A. Shteinman, E.V. Starokon, G.I. Panov, J. Catal. 207 (2002) 341.
[15] L. Guczi, K. Lázár, React. Kinet. Catal. Lett. 96 (2009) 335.
[16] J.B. Taboada, E.J.M. Hensen, I.W.C.E. Arends, G. Mul, A.R. Overweg, Catal. Today 110 (2005) 221.
[17] M. Schwarze, Z. Sobalík, Z. Tvarůžková, E.G. Caspary, D. Nižnanský, Czechoslovak J. Phys. 56 (Suppl. E) (2006) E147.
[18] K. Lázár, G. Lejeune, R.K. Ahedi, S.S. Shevade, A.N. Kotashane, J. Phys. Chem. B 102 (1998) 4865.
[19] E. Ivanova, M. Mihaylov, K. Hadjiivanov, V. Blasin-Aubǐe, O. Marie, A. Plesniar, M. Daturi, Appl. Catal. B 93 (2010) 325.
[20] V. Blasin-Aubé, O. Marie, J. Saussey, A. Plesniar, M. Daturi, N. Nguyen, C. Hamon, M. Mihaylov, E. Ivanova, K. Hadjiivanov, J. Phys. Chem. C 113 (2009) 8387.
[21] Z. Sobalík, J. Dědeček, D. Kaucký, B. Wichterlová, L. Drozdová, R. Prins, J. Catal. 194 (2000) 330.
[22] E. Kuzmann, S. Nagy, A. Vértes, Pure Appl. Chem. 75 (2003) 801.